Seismic Analysis of the Stevenson Bridge

Photo of Stevenson Bridge, looking north

By
Caleb Stewart
MS Plan II Report

Department of Civil & Environmental Engineering
University of California, Davis

December 13, 2013

Table of Contents

I. Abstract

The purpose of this report is to analyze the seismic response of the Stevenson Bridge in Yolo County, California from a design-level seismic event. By modeling each bridge footing using site-specific soil properties with the finite element analysis software ABAQUS, the equivalent spring constants in each of the orthogonal translation and rotation degrees of freedom were calculated. Direction-specific ground acceleration time histories from three site-similar earthquakes were scaled to match the recommended site-specific spectrum provided by a geotechnical report (Kleinfelder 2006). The equivalent footing spring constants and scaled ground motion data were applied to a model of the bridge in SAP2000, and using non-linear structural analysis, the bridge response time history was determined. The resulting stresses, displacements, and reactions were used to characterize the response of the bridge to the seismic event.

II. Background

Stevenson Bridge is a double tied-arch reinforced concrete bridge spanning Putah Creek in Yolo County, just north of the Yolo/Solano county border and is situated among the agricultural fields between Davis and Winters. It is narrowly wide enough for two passenger vehicles, and known locally as "Graffiti Bridge" from the layers of colorful graffiti covering much of the bridge, it is used primarily by tourists, bicyclists, locals, and for agricultural traffic. Built in the mid-1920s, it is classified as a "Historically

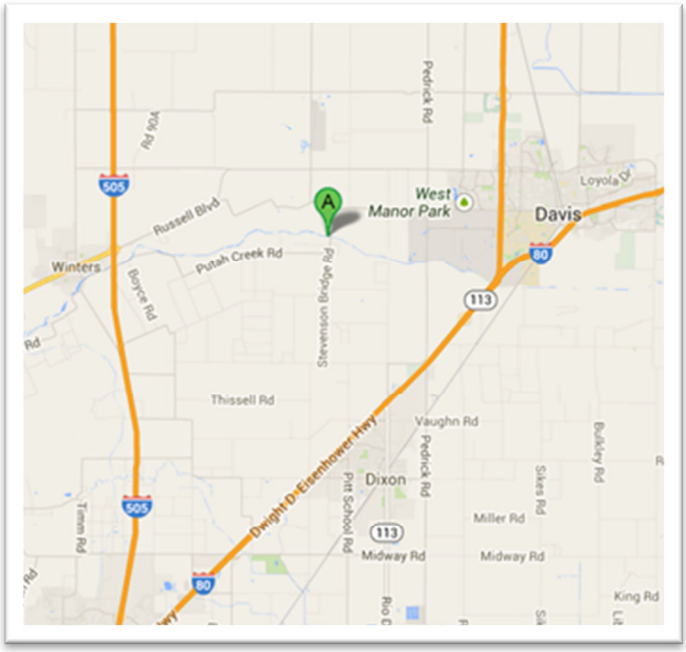

Figure 1: Location of Stevenson Bridge

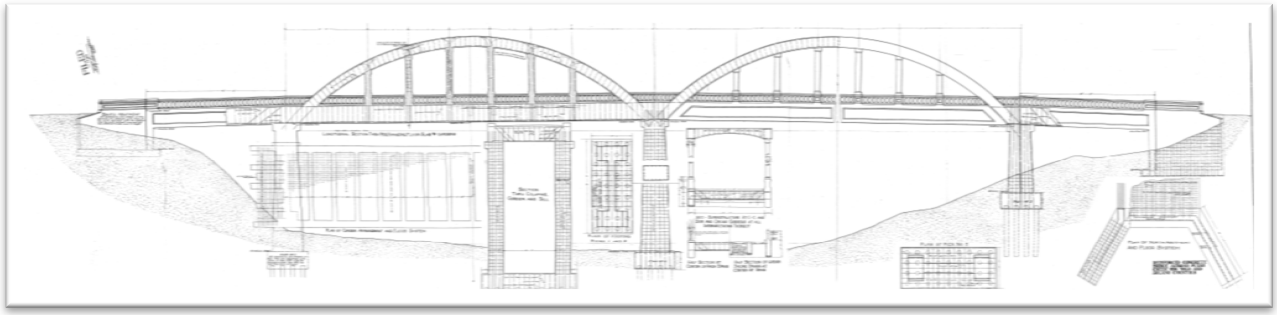

Figure 2: Original 1923 structural plans of Stevenson Bridge

Significant Bridge," and has not been retrofitted nor sustained any significant structural damage, however, a significant amount of scour, or water erosion around the footings, has occurred.

Overall, it is approximately 350 feet long over two abutments and four spans, oriented in a NNW direction. The 40-ft long end spans are concrete slab-on-girder, with two 108-ft tied-arch spans between. The abutments, located near the top of the river bank, have wing walls supported by spread footings to retain the soil. The bridge spans are supported by three concrete piers across the creek channel with spread footings on top of 40-ft deep wood piles at the southern and middle pier, and 15-ft deep reinforced concrete piles at the northern pier with 36 piles in each pier footing. As with the rest of the Sacramento Valley, the bridge site upper layer of soil consists of quaternary alluvium. Test boreholes drilled at the bridge location indicate alternating layers of silts, clays, gravels and sands to 100-ft deep from the surrounding valley level. The site is located about 6 miles from the nearest fault zone, the Coast Ranges-Sierran Block (Kleinfelder) as shown in Figure 3, which are oriented roughly parallel to the bridge. Existing reports on the bridge

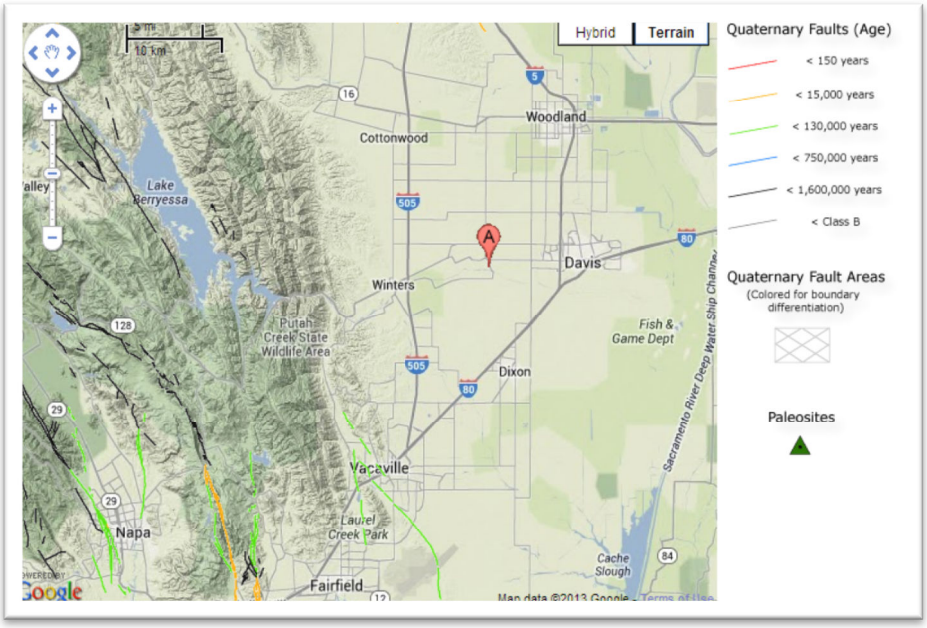

Figure 3: Bridge location with respect to nearest seismic faults

include routine Caltrans inspections, a 2006 geotechnical report by Kleinfelder, a 2007 structural analysis and recommendations report by Imbsen (formerly TRC Imbsen). Caltrans has listed the bridge as structurally obsolete due to the narrow width and difficult vehicular lane geometry, as well as scour-critical due to the erosion at the footings. Concrete cracking and spalling has occurred and has exposed steel reinforcement in a number of places.

The following sections describe the procedure and results from the footing analysis, scaled ground motion data, and overall structural non-linear analysis to determine the seismic structural response of the bridge.

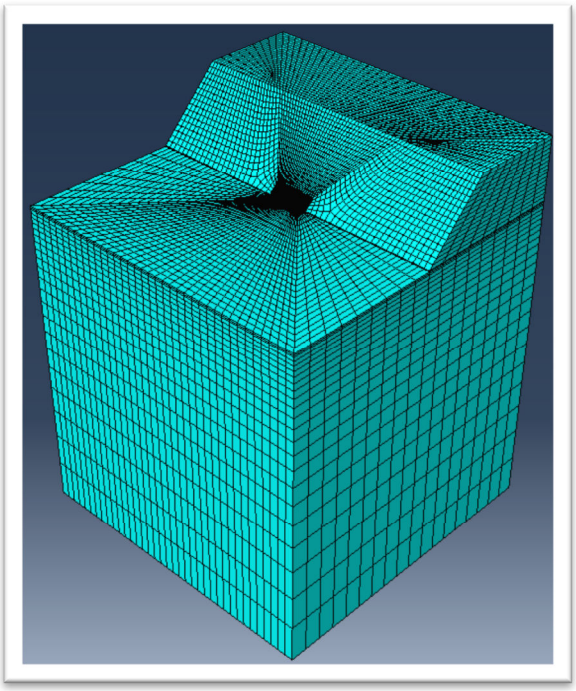

Overall soil field at south pier

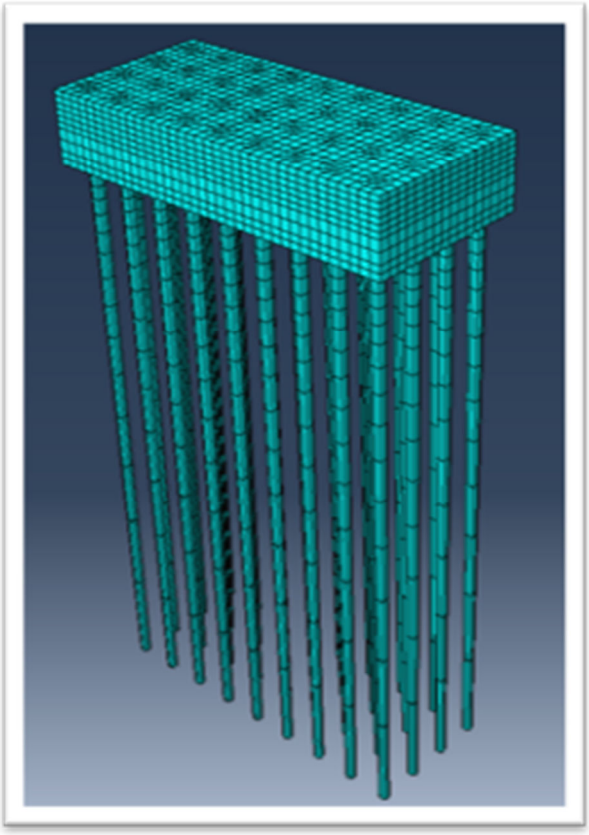

Footing model at middle pier

Figure 4: ABAQUS Models

III. Footing Analysis

a. Footing Models

Each unique footing was modeled in ABAQUS and subjected to static loads to determine the overall footing spring constants in all six orthogonal directions. The models (the south pier is shown in Figure 4) include the footings situated in a roughly 200-ft soil field on all edges to minimize the effect of near-footing boundary conditions. The meshes contain up to 274,000 elements, with

an approximate mesh size of 6 inches close to the pier, radiating outward. The variation in size of the elements was to maximize accuracy at the point of interest while maintaining computing efficiency with a minimum number of elements.

b. Material models

Three materials were used in the ABAQUS model: concrete, wood, and soil. Concrete was defined as a homogeneous elastic material, wood was defined as an orthotropic elastic material, and the soil was defined with isotropic elasticity and Mohr-Coulomb plasticity varying with depth. The following subsections elaborate on the material properties of each.

i. Concrete

The modulus of elasticity for concrete was taken from ACI-318 05 as $E_c = 57000\sqrt{f_c'}$, where $f_c' = 2500$ as taken conservatively from the average from rebound hammer tests and cored sample compression tests performed by Kleinfelder. No reinforcement or failure criteria were included in the concrete model.

ii. Wood

Since wood is an orthotropically elastic material, an elasticity matrix was generated using test data from the USDA Wood Handbook, 2010 using Douglas Fir Interior West at 12% moisture. Using a cylindrical coordinate system and the provided definition of an orthogonally elastic matrix from ABAQUS, the calculated orthotropic elasticity matrix calculated is shown in Table 1. A failure criterion was not included for the wood material in this analysis.

Table 1: Orthotropic variables for ABAQUS

D Matrix (psi)

143892	64278	38961	0	0	0
	109194	33849	0	0	0
		1916761	0	0	0
			11627	0	0
	SYM			106304	0
					129558

iii. Soil

The geotechnical report provided by Kleinfelder includes soil engineering properties, strata and standard penetration tests for two 100-ft deep boreholes at each end of the bridge. NovoSPT software was used to correlate the SPT values (taken every 5 feet in each borehole) to the modulus of elasticity and friction angle of the soil. The modulus of elasticity correlation was performed using the correlations shown in Figure 5 for Borehole 1, and converted to psi for use in ABAQUS. To define the soil friction angle, NovoSPT was used with the correlation from Shioi and Fukui (1954), as it matched expected values of clay friction angle and the measured values of the friction angle of sand per Kleinfelder.

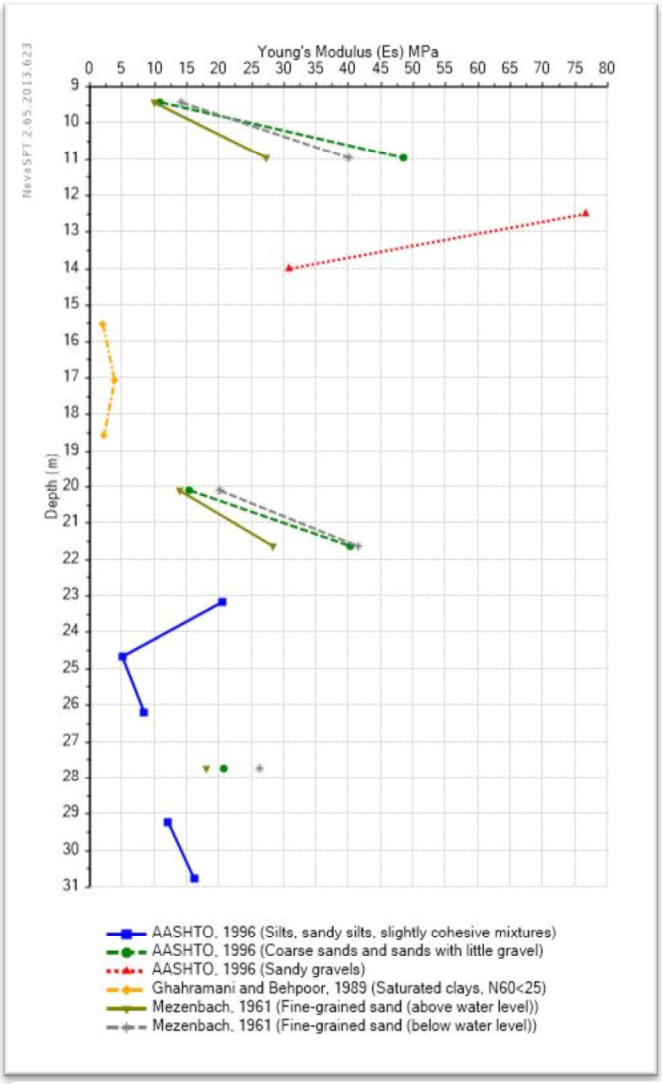

Figure 5: NovoSPT correlation for soil modulus of elasticity

With the modulus of elasticity, friction angles, cohesion, and angle of dilation determined for each soil depth increment up to 100 feet deep, a linear trendline was established to roughly estimate the soil material properties between the bottom of the borehole to the full 200-ft depth of the ABAQUS model. All these values were input into ABAQUS and using the UFIELD subroutine with a Fortran and C++ compiler, the variation of soil properties with depth was interpolated to the integration points of the mesh in the soil field.

c. Loading and Boundary Conditions

To model the soil field as accurately as possible, the far-field side boundary conditions were prescribed as zero translation in the horizontal direction, and the bottom as zero translation in the vertical direction. This was to allow the soil field to "squash" as it deformed along the edges of the bounding box under a gravity load, and resist lateral deformation when the footing loads were applied.

The footing loading was initialized with gravity and the full dead weight of the bridge at that footing location before any incremental loading was applied in subsequent steps. With each incremental load, the deflection of the footing was measured for each degree of freedom for each loading case. Figure 6 shows the force – displacement and the moment-angle graph for the south pier. Due to the linearity of the results, the equivalent spring constants were calculated using the approximate average of the slope of the curves, as graphically represented in Figure 7.

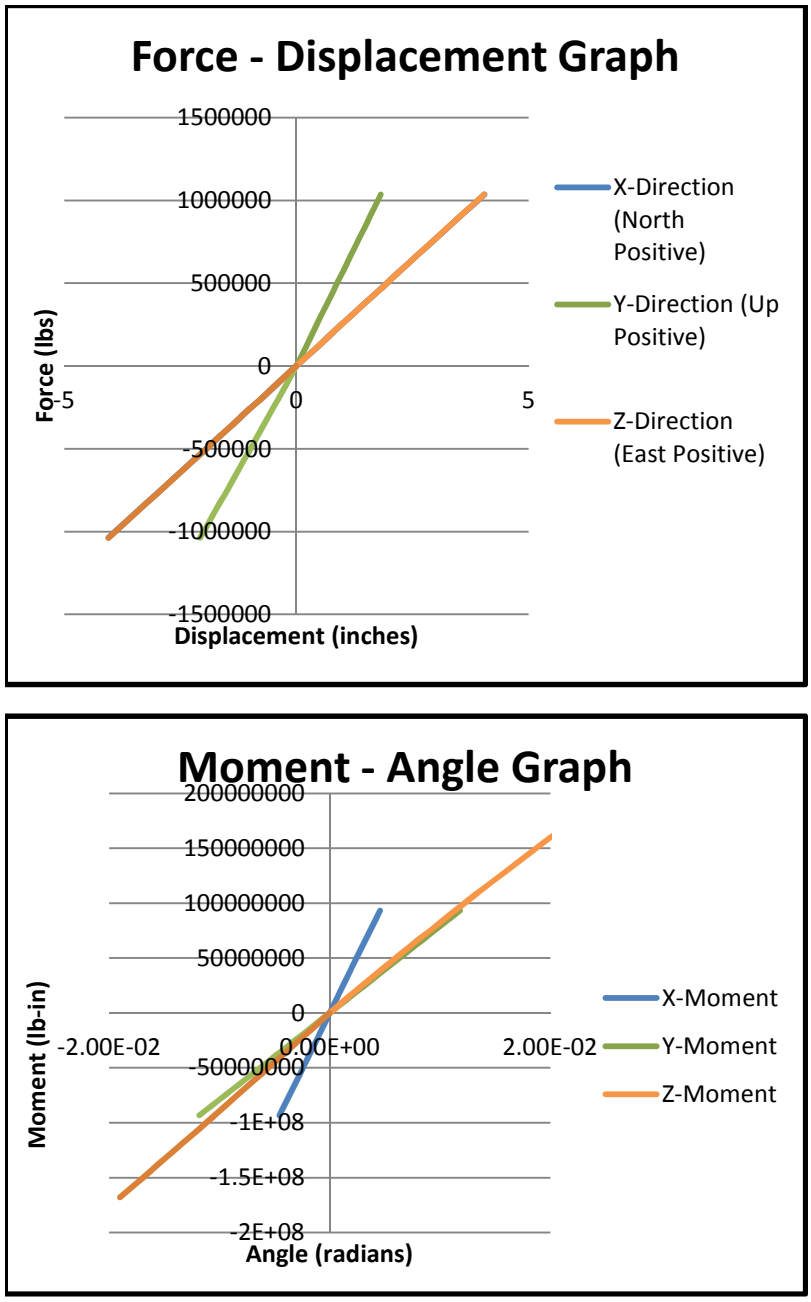

Figure 6: Force – displacement and moment – rotation angle graphs for the south footing

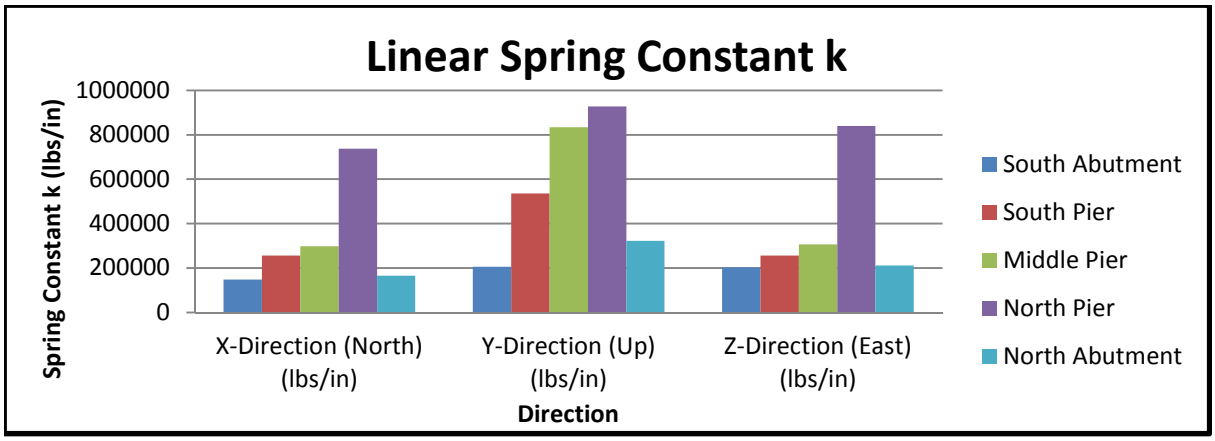

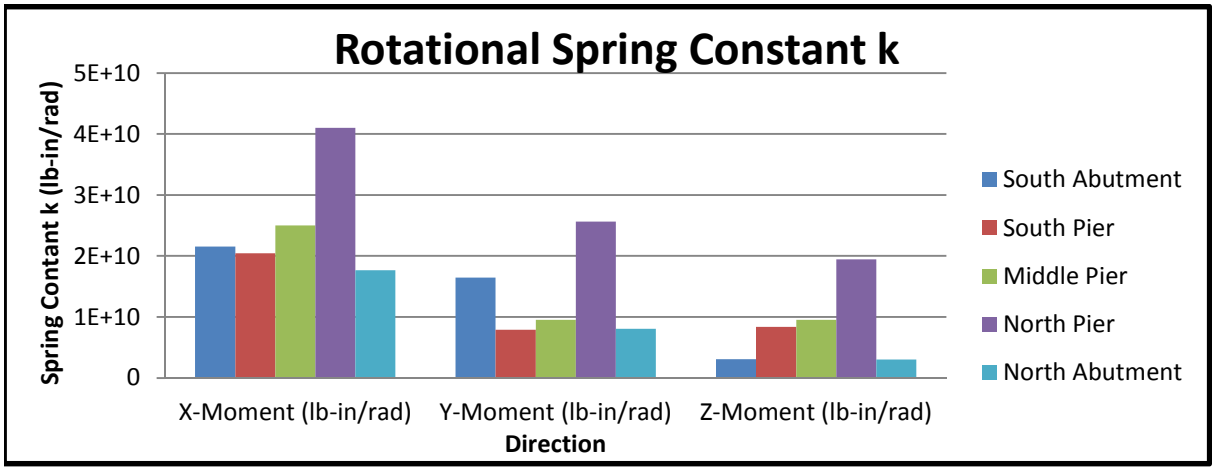

Figure 7: Charts comparing linear and rotational spring constants for all footings

IV. Ground Motion Data

a. Earthquake selection

Following the guidelines of the 2012 AASHTO LRFD Bridge Design Specifications, three ground motions were selected and scaled to meet the target site-specific spectrum provided by Kleinfelder geotechnical report. To select the desired ground motions, several site-similar ground motion recorders that had recorded significant earthquakes were selected as candidates from the Center for Engineering Strong Motion Data website. The earthquakes were mapped to their recording stations, as shown in Figure 8. Three earthquakes, each from different directions from the epicenter to the recorder, were selected to capture the varying effects of wave direction propagation. The final earthquakes were selected based on close proximity of the epicenter to the

recorder, and are indicated by the red lines in Figure 8. The northern-most earthquake was a magnitude 3.9 from Napa in 2008, the middle earthquake was a magnitude 5.9 from Livermore in 1980, and the southern-most earthquake was a magnitude 6.5 from Coalinga in 1983. See Figures 9-11 for the unscaled ground motions from the Center for Engineering Strong Motion Data Website.

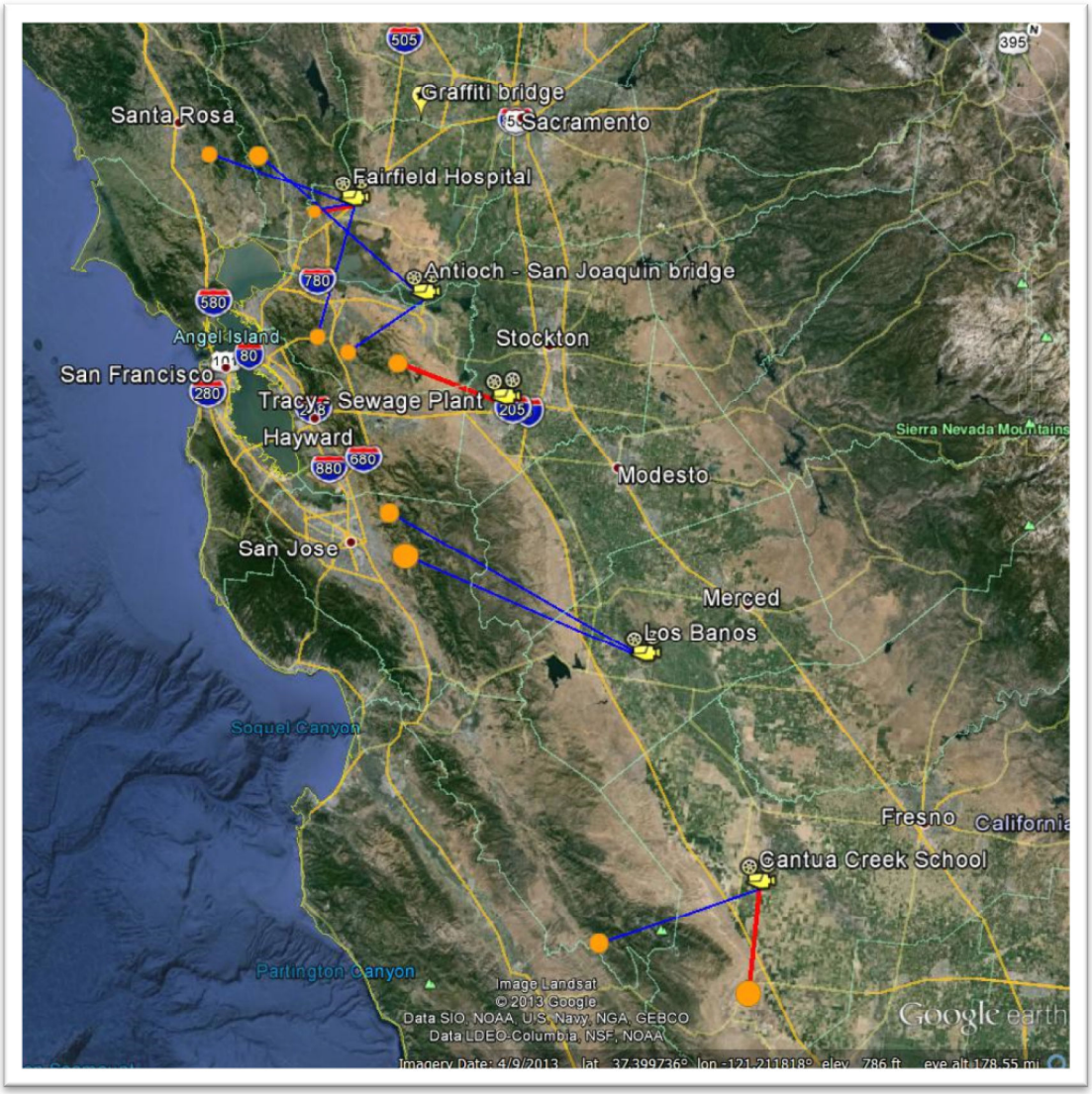

Figure 8: Map of earthquakes (orange circles), recording stations (camera icon), and the direction and distance from the earthquakes to the recording station (blue and red lines; red lines represent data selected for analysis). Note bridge site at northern end of figure.

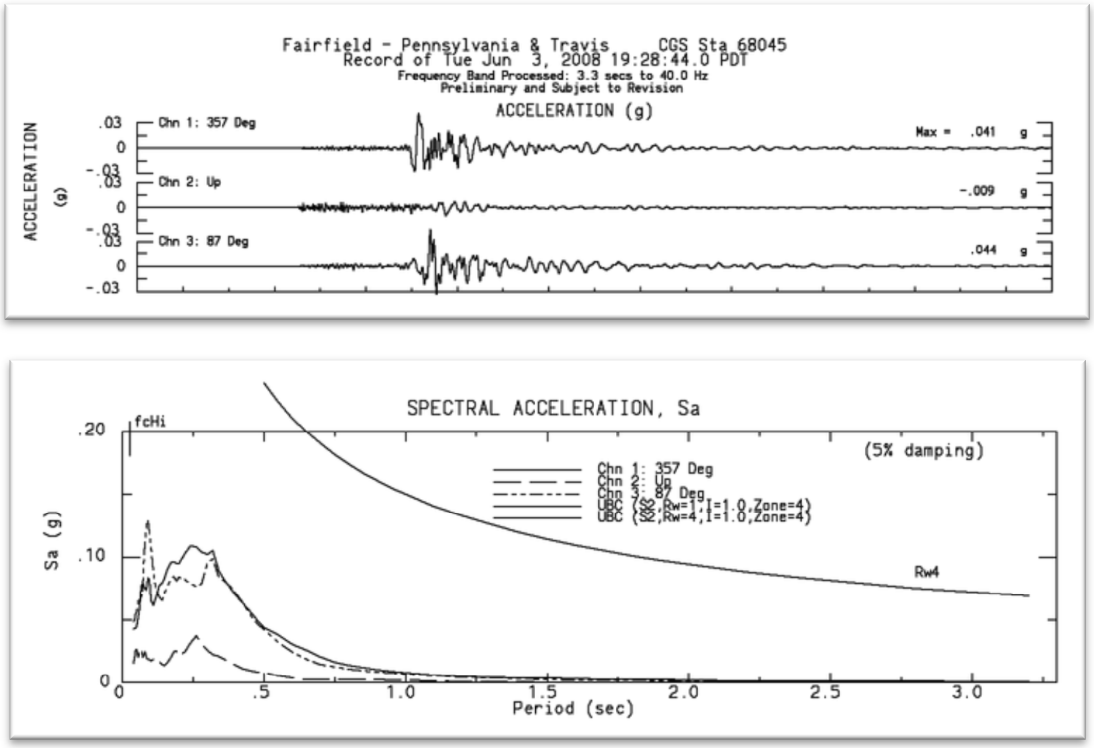

Figure 9: Ground acceleration and response spectra recordings of M3.9 Napa Earthquake

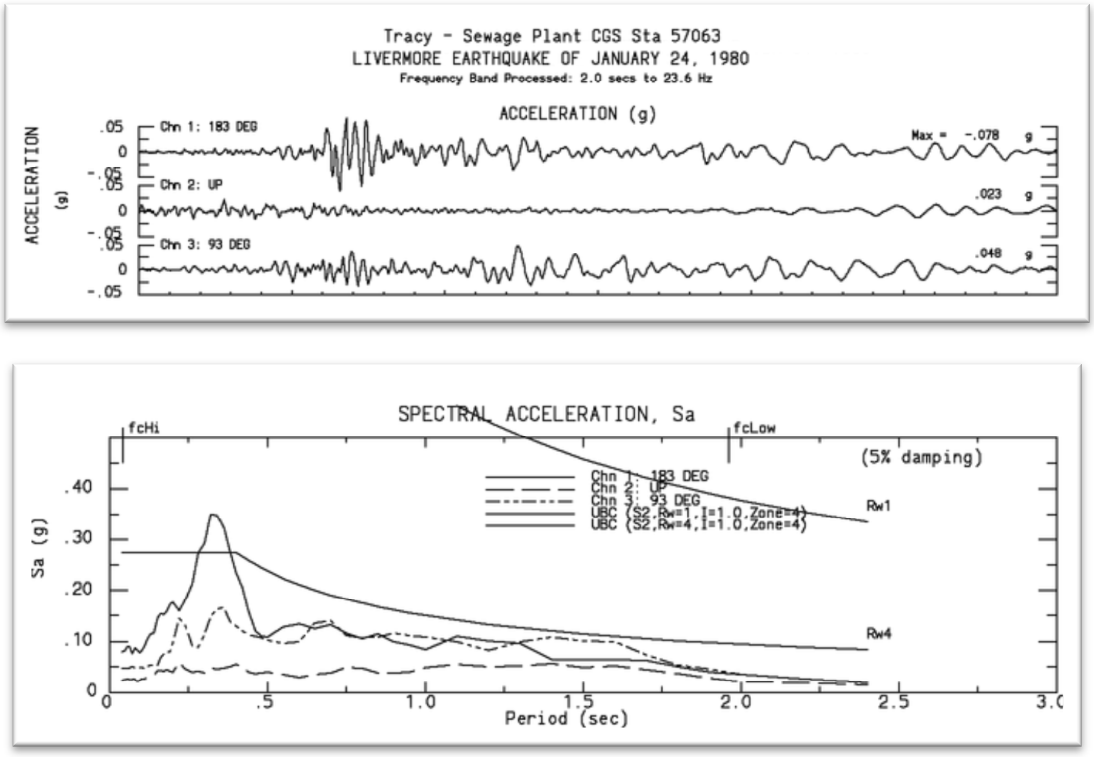

Figure 10: Ground acceleration and response spectra recordings of M5.9 Livermore Earthquake

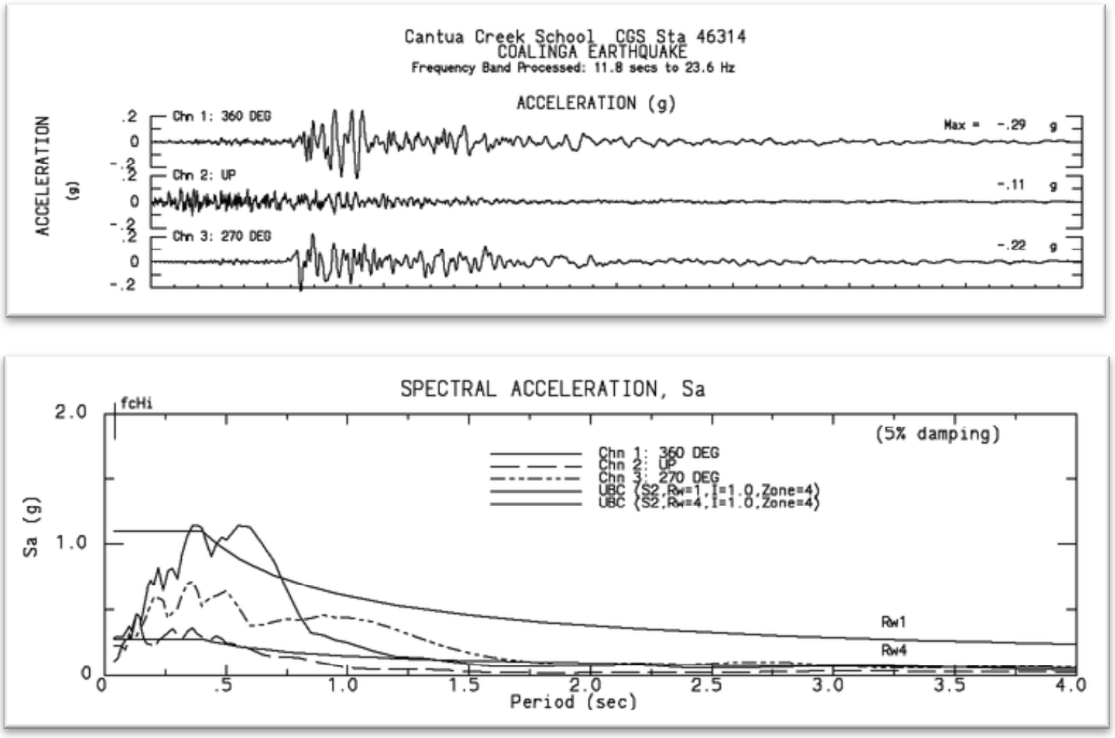

Figure 11: Ground acceleration and response spectra recordings of M6.5 Coalinga Earthquake

b. Earthquake scaling

The earthquake data were obtained from two sources and required manipulation from each to match the target site-specific ground motion response spectrum provided by the geotechnical report by Kleinfelder (see Figure 13). The raw ground motion data were scaled to match this target spectrum in two different ways. The first data source, the Pacific Earthquake Engineering Research Center, provides

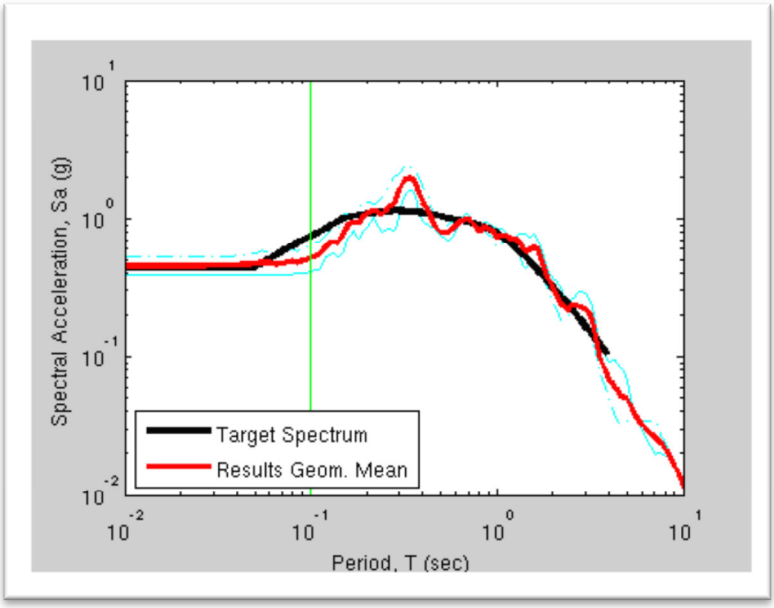

Figure 12: PEER - scaled spectra from the M5.9 1980 Livermore earthquake

ground motion data rotated to fault-normal (FN) and fault-parallel (FP) directions, and scales the ground motion to match a target spectrum (see Figure 12). The M5.9 and M6.5 earthquake ground motions were obtained from PEER.

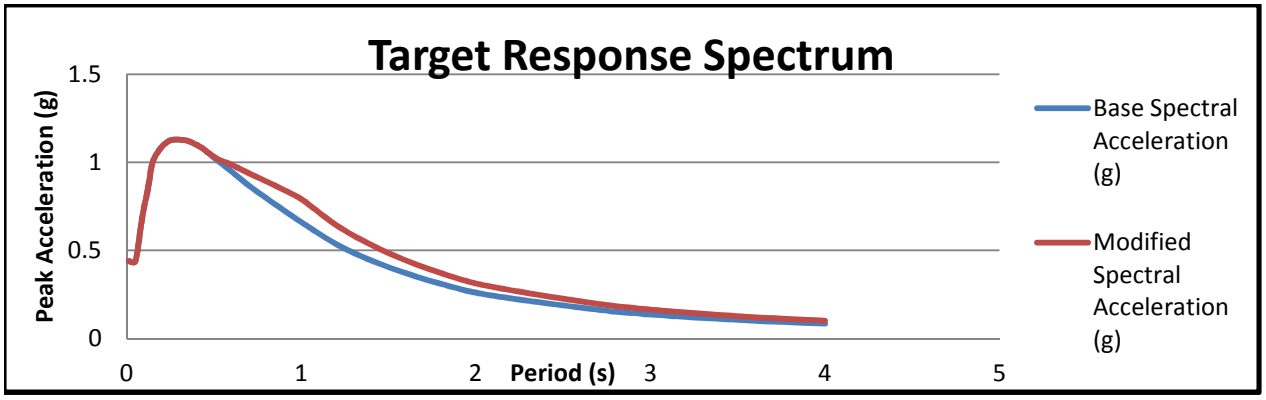

Figure 13: Target response spectrum provided by Kleinfelder

Since the M3.9 earthquake was not available from the PEER website, Microsoft Excel was used to rotate horizontal ground motions 12° counterclockwise using basic trigonometry to match the fault-normal and fault-perpendicular ground motions provided by PEER. The FN and FP directions were convenient because the bridge is oriented parallel to the nearest fault system. See Figure 14 for example original and rotated ground motion for the north-direction.

With the rotated ground motion, the computer program Bispec was used to create a bidirectional spectrum of the rotated ground motion, as shown in Figure 15. The bidirectional response spectrum was used to calculate the scale factor of 10.4 to match the peak of the target spectrum. Although the peak of the scaled data matched the peak of the target spectrum, this

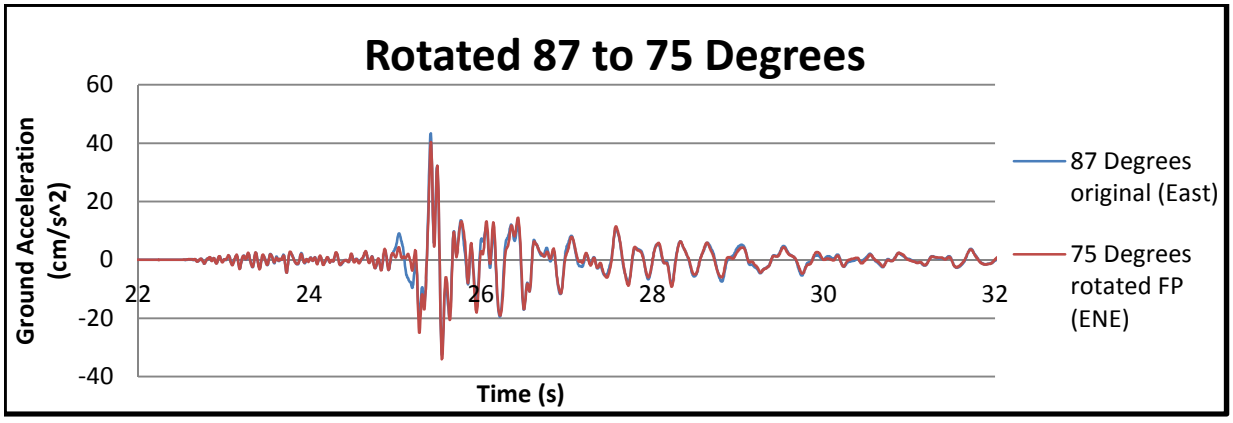

Figure 14: Rotated ground acceleration from the M3.9 earthquake, eastern direction

ground motion response spectrum inadequately matched the longer period target spectra, as discussed in in the results.

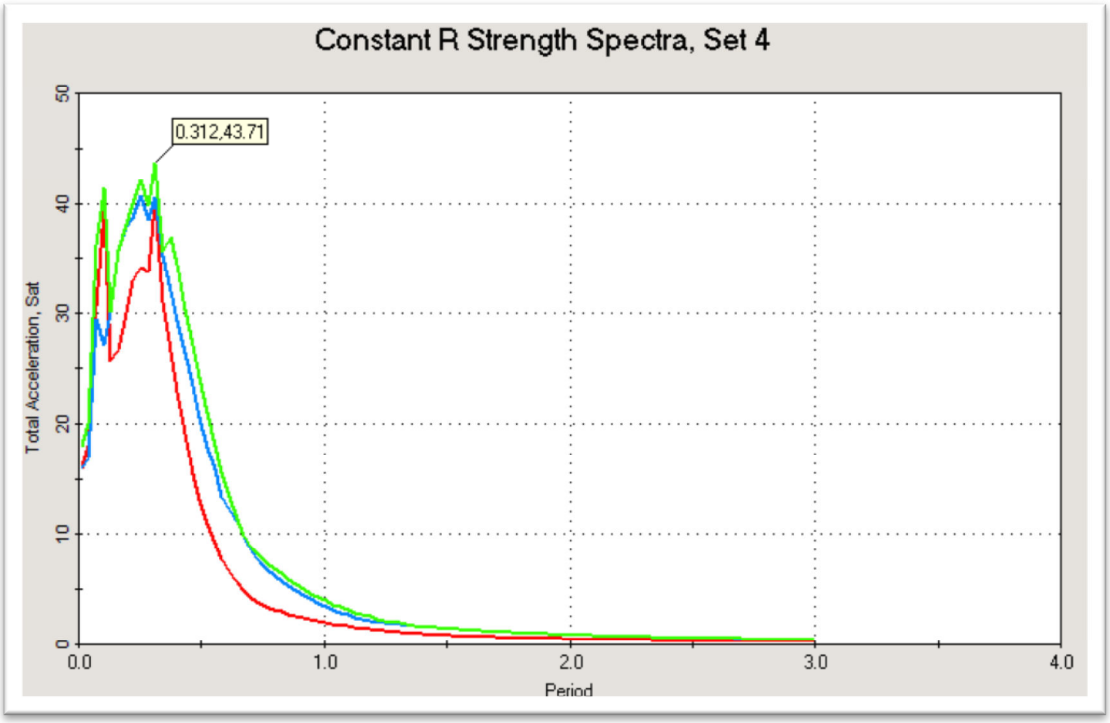

Figure 15: M3.9 Ground motion spectra from rotated orthogonal angles (red is eastern direction, blue is northern direction), and bidirectional analysis (shown green). Units are in inches and seconds.

V. SAP2000 Analysis

a. Model Definition & Loading

Using the original structural plans, the bridge was modeled using SAP2000. Member sizes & reinforcing were designed as shown on the original plans, and the footing restraints used the spring constants derived from the ABAQUS analysis. The reinforcing steel was determined to be

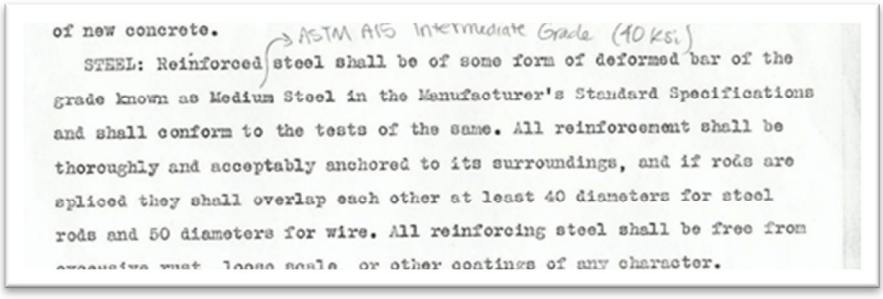
of new concrete.
STEEL: Reinforced steel shall be of some form of deformed bar of the grade known as Medium Steel in the Manufacturer's Standard Specifications and shall conform to the tests of the same. All reinforcement shall be thoroughly and acceptably anchored to its surroundings, and if rods are spliced they shall overlap each other at least 40 diameters for steel rods and 50 diameters for wire. All reinforcing steel shall be free from

Figure 16: Original construction specifications for steel grade

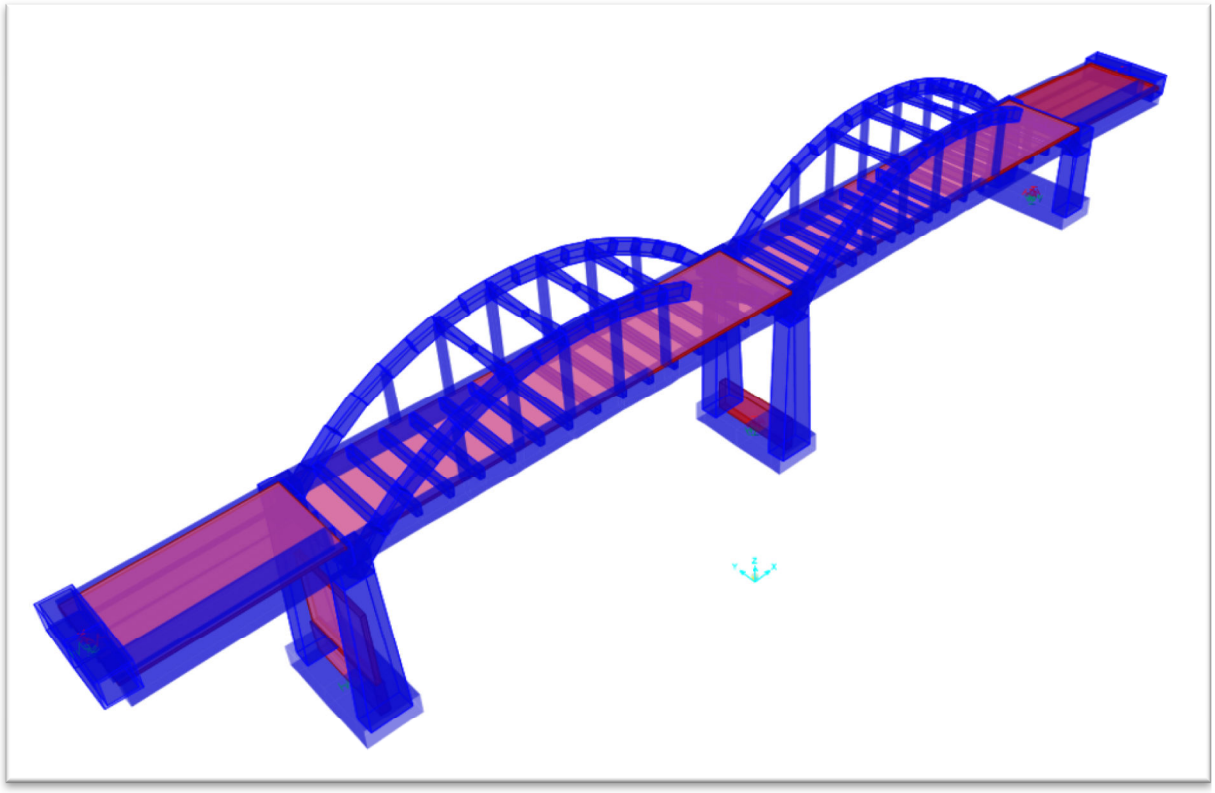

Figure 17: SAP2000 model of Stevenson Bridge

Gr. 40 steel from the original construction documents (Figure 16), and the concrete material used was 2500 psi, unconfined. Both materials used the default SAP2000 non-linear stress strain curve. The abutment footings were modeled using large steel tubes with a zero mass multiplier designed to act rigidly, to which the spring constants were applied. The pier footings were modeled as their actual size to include the dynamic properties and self-weight of the footings in the analysis, with the spring constants applied at the middle of the piers. The deck was created as integral with the beam girders with the appropriate offset from the centerline of the girders. The moment of inertia for the pier columns was reduced by 0.5 to determine the period as required per AASHTO Bridge Design Specifications section C4.7.1.3. See Figure 17 for the SAP2000 bridge design.

The scaled and rotated ground acceleration spectra were added to the model as a multi-directional simultaneous non-linear time history analysis. The fault-parallel motion was applied in the longitudinal direction of the bridge, with the fault-normal motion applied perpendicularly to the bridge. The up-direction scaled ground motion, along with the incremental gravity loading (constant G), were also simultaneously applied. No other loads were considered in the analysis.

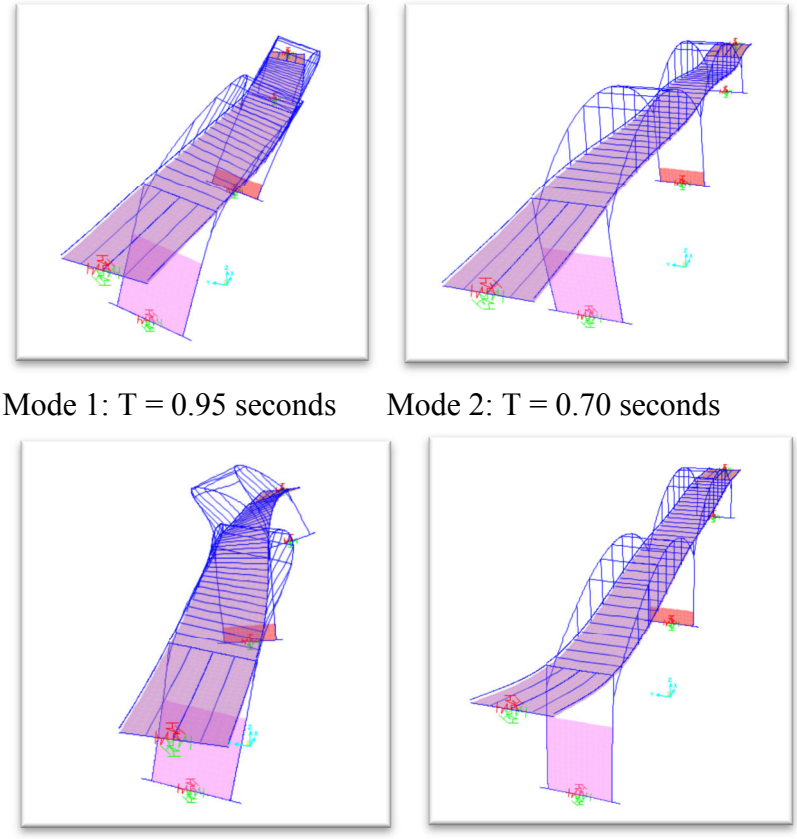

Mode 1: T = 0.95 seconds Mode 2: T = 0.70 seconds

Mode 3: T = 0.52 seconds Mode 4: T = 0.51 seconds

Figure 18: Mode shapes and period times

b. Analysis Results

The modal responses of the first four modes are shown in Figure 18. The time history response for top of the middle concrete pier in the perpendicular direction to the bridge is shown in Figure 19 for all three earthquakes. Because the M6.5 earthquake created the greatest displacement of the bridge, this is the governing case of the three bridges and must be used for analysis per AASHTO. The envelope axial force, S11 stress, and bending moments are shown in Figure 20 for the M6.5 earthquake.

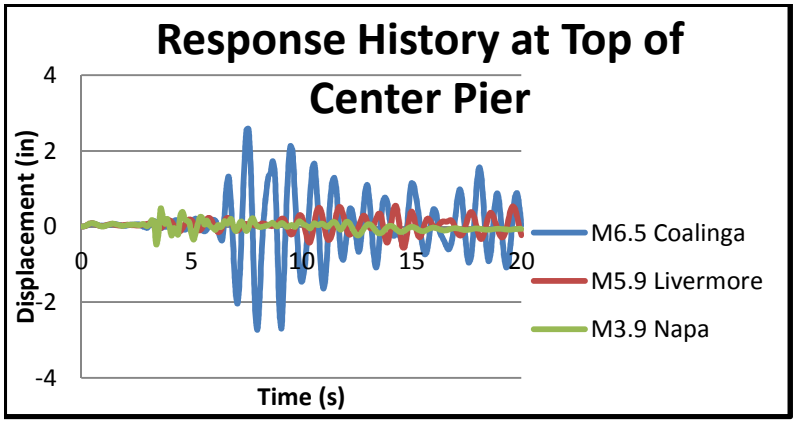

Figure 19: Response time history at top of center pier

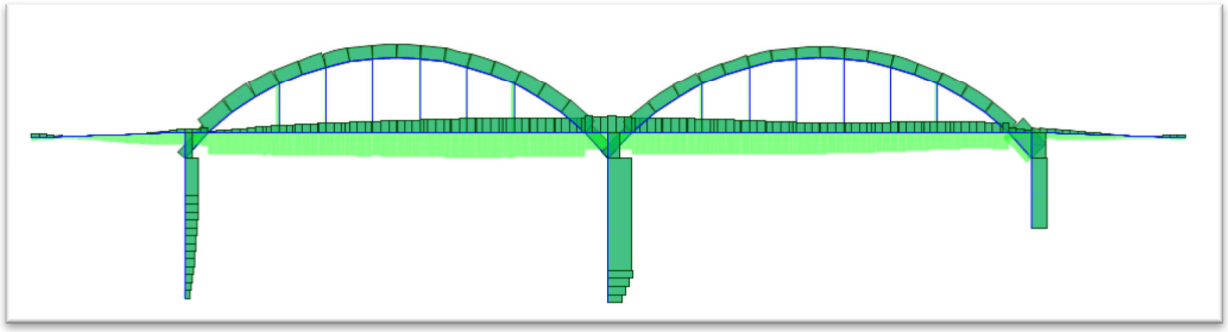

Axial force envelope diagram

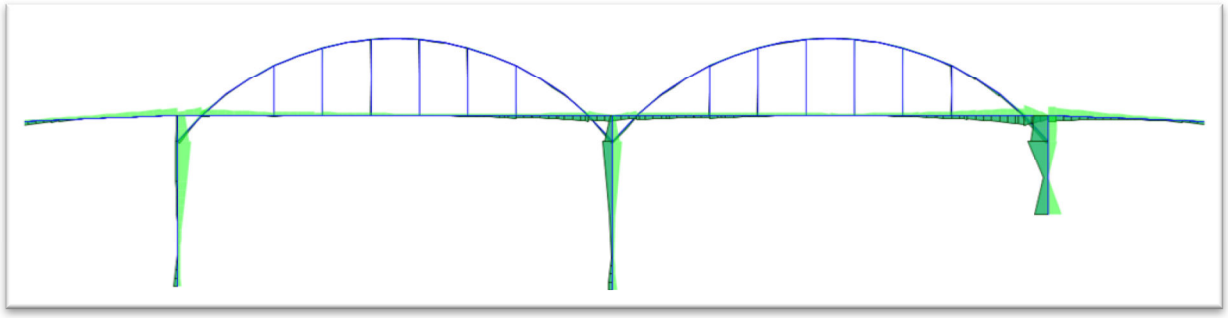

Major-axis moment envelope diagram

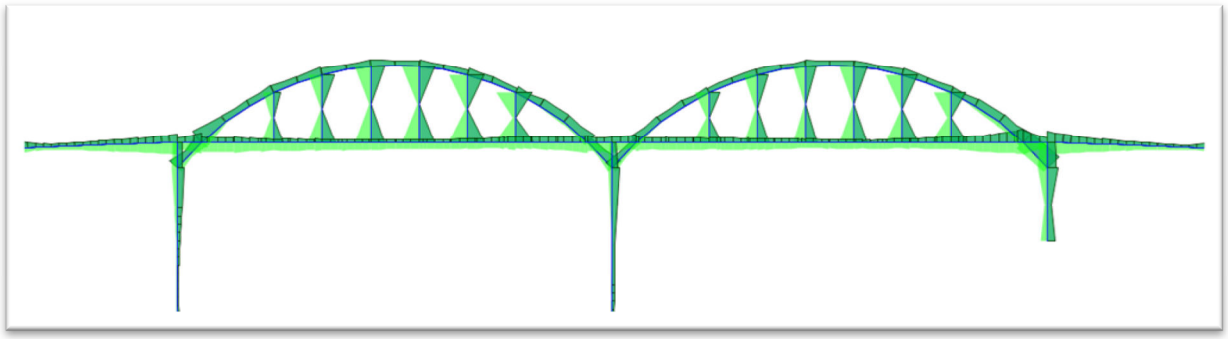

S11 Max/min stress diagram

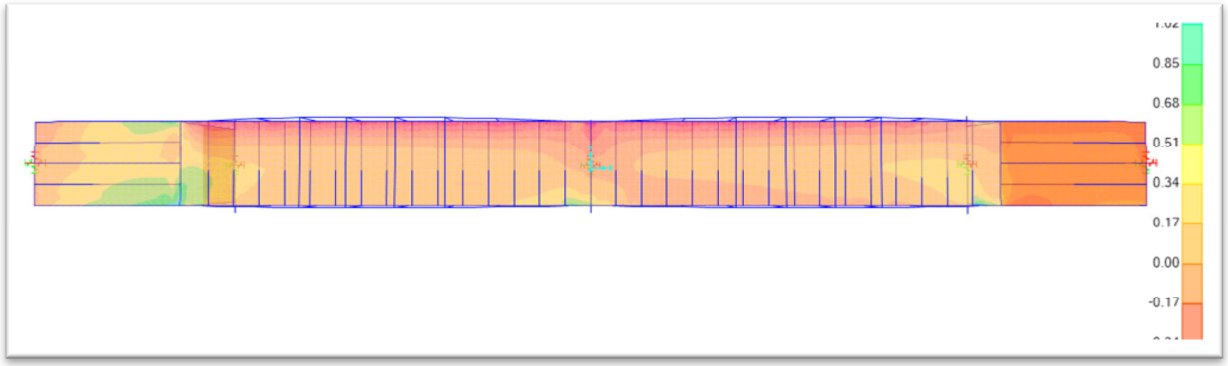

Stress in concrete deck at maximum lateral deck displacement (top view)
Figure 20: Force diagrams in structure

VI. Discussion

a. Soil Properties

The largest potential source of error in the analysis likely stems from correlating standard penetration tests and soil type to modulus of elasticity, friction angle, and cohesion. Using the correlation software NovoSPT, the standard penetration blow count and soil strata were correlated to the resulting data using up to 100 soil studies. From the resulting correlations, it was observed that there existed a wide variability in results, with some results calculated as high as five times other results. However, using the guidelines from suggested material properties ("Some Useful Numbers"), erroneous data were removed to determine a final correlation. Another likely source of error is from the soil modeled as isotropically elastic. Because soil is an orthotropic material, inclusion of the orthotropic nature would have affected the footing spring constants. While error in the results of the soil is expected, it is believed that the resulting soil data will be adequate for use in ABAQUS.

b. ABAQUS Analysis

A static analysis was performed in ABAQUS to determine the spring constants of the footing. Although a dynamic analysis would realistically better capture the dynamic footing-soil interaction, the resulting force-displacement curve would have been time-rate dependent, adding a degree of complexity to the analysis, and due to the likely error already present in the soil properties, the use of a dynamic analysis was unwarranted.

Incremental loads were selected that were expected to exceed the seismic loads on the footing to accurately model the force-displacement curve. However, while a small amount of plastic deformation occurred in the soil, the overall force-displacement curve was largely linear, so linear spring constants were calculated for use in SAP2000. Had the footings appreciably deformed plastically, nonlinear springs would have been used in the bridge analysis.

Another potential source of error in the ABAQUS analysis was the use of distorted elements, or elements exceeding an ideal geometry (e.g., long slender or flat hex elements where a cube shape is ideal). While most elements were not distorted, up to roughly 5% of the elements triggered a distorted element flag in ABAQUS. Unusual deformation at these elements, however, was not apparent after the analysis.

Computationally speaking, the amount of analysis time for the footings (up to 4 hours per degree of freedom per footing) was excessive when considering the uncertainty of the input soil data. Despite this, the overall spring constants calculated were likely relatively similar to the actual response of the footings. To perfectly capture the spring constant in each orthogonal direction, the footing should be restrained in movement in all other degrees of freedom except the one measured. However, for simplicity, the boundary conditions were held only at the far edges of the soil field and the loads in each orthogonal direction were applied. Significant deformation into the other degrees of translational and rotational freedom was not observed.

Finally, another potential source of error was likely due to the Mohr-Coulomb failure criteria in the soil. The ABAQUS program experienced convergence errors when the soil cohesion was set at less than 2 pounds per square inch. This cohesion was included at the interface between materials, and would have caused a small error at the pier footings and a larger error at the abutments. Poor convergence was remedied by specifying an unsymmetrical solver matrix with an iterative solver, yet a minimum cohesion was required to avoid convergence errors.

c. Ground Motion Scaling

Selection, manipulation, and ground motion scaling revealed strengths and weaknesses of the ground motions selected. Since the geotechnical report included a site-specific target spectrum, scaling to match the peak of the spectrum was straightforward. However, due to variations in the selected ground motion response spectra, the M6.5 scaled earthquake spectrum matched the target spectrum much more closely than the M3.9 spectrum. Although AASHTO requires three distinct earthquake time histories that have a spectrum that closely matches the target spectrum, due to the limited amount of strong-motion data from site-similar seismographs, only one earthquake (M6.5) provided data that closely matched the target spectra. This earthquake was distinguished from the others because of its large peak accelerations for longer periods.

The amount of scaling required to meet the target spectrum varied greatly. For the M6.9 earthquake, the spectrum was scaled likely less than 1.5 times the original ground motion (as evident by a strong spectrum of the unscaled ground motion). However, although the M3.9 earthquake was twice as close as the M6.5 to the recording station, the M3.9 earthquake needed to be scaled about 10 times to meet the target spectrum. The M6.5 earthquake provided a quality

ground acceleration time history for use in SAP2000, and was subsequently used as the controlling seismic event, as will be discussed in the following section.

d. SAP2000 Analysis

Because this bridge had a fairly long mode 1 period (nearly 1 second), the magnitude 6.5 earthquake created much greater displacements than the other two earthquake time histories. Observation of the spectra of the M6.5 earthquake reveals that peak accelerations are much greater in the longer periods than the other two spectra, highlighting the difference of a large versus small earthquake despite both spectra being scaled to the peak of the target spectrum. For structures with a mode 1 period of about 0.3 seconds, any of these scaled ground motion data would have likely have been satisfactory for the structural analysis.

From the analysis time history, the peak displacement of the top of the pier from the M6.5 earthquake was less than three inches, or roughly 0.5%. This indicates a substantial stiffness and ability of the bridge stiffness to resist a large seismic event. However, shortcomings in the SAP2000 analysis include lack of a progressive concrete degradation model, and lack of an output to display yielding of concrete elements and time-history non-linear strain response for each element.

For a thorough analysis on the concrete degradation and steel yielding, a different program or further data manipulation would be required. The concrete structure design/check feature of SAP2000 is useful for scaled ground motions to a response coefficient, or R-value. R-values vary depending on the bridge component from 1.5 to 5.0. Because the R-value allows for the reduction of design force due to expected ductility in concrete members, a scaled down time-history analysis would be required to check each component with its corresponding R-value to satisfy the code design requirements. By applying the full seismic force on the structure, the structural members are expected to yield significantly. However, without the functionality to display the extent of yielding in SAP2000, a moment-curvature and concrete-steel degradation model could be implemented to verify the concrete condition after this seismic event. Finally, although physical testing on the bridge has indicated an average concrete compressive strength of roughly 2900 psi, and that all members contain reinforcing ties, the concrete was modeled as unconfined as opposed to the Mander's Model of confined concrete, which was stiffer and was able to sustain greater compressive stress.

e. General Considerations

A number of structural issues were unaccounted for in this analysis. First, some amount of spalling has occurred, exposing reinforcement in a number of places on the bridge. These areas will experience reduced member capacity, which was not captured in the SAP2000 analysis. Furthermore, an extensive member capacity and weak area investigation in SAP2000 was not performed. Another potential source of error is the difference between the plans and the as-built conditions. The south abutment had a large concrete footing under the footing that was not shown on the original structural plans plans. This was accounted for in the ABAQUS model by incorporating the estimated the footing size, yet the actual extent of the footing was unknown. Also, expansion joints called out on plans were not apparent in the field investigation, and reinforcing through construction joints, particularly at the abutments, was unknown. The ABAQUS analysis was performed with the assumption of full structural fixity to the footings. Also, no expansion joints were observed in the field investigation, though shown on the plans. In terms of structural accuracy, all members except the slab deck were modeled with the correct reinforcing in SAP2000, except that the amount of reinforcing steel in the concrete deck cannot be specified due to program limitations. While concrete cover and reinforcing steel grade can be specified, SAP2000 automatically calculates the stiffness of the slab, regardless of the amount of actual reinforcing in the physical model.

The footing spring constants used, derived from ABAQUS using material data from correlation software, may have been better determined using a specialized footing software to reduce the amount of uncertainty, as well as reducing modeling and computational time. It is noteworthy that the spring constants applied to the footings nearly doubled the first period time of the bridge versus fixed footing conditions.

The footings supported by wood piles experienced a lateral force of up to 350 kips. A quick calculation suggests that if these piles are in good condition (not decayed), they should be able to resist the lateral seismic forces without shearing off. However, due to the age of the bridge and proximity of the wood piles to the surface of the ground, it is likely that the wood piles have experienced some degree of decay.

VII. Conclusions

While this report investigated the response of the bridge to direction-specific scaled motion, no conclusions can be currently drawn whether or not the bridge will survive a design-level earthquake. Further detailed analysis is required. Should the full unscaled ground motion be applied to the analysis model, the yielding and damage sustained to the concrete members must be investigated. Alternatively, using a reduced ground motion based on the response factor R, the capacity of the members to resist the reduced static equivalent load must be investigated. Consideration should also be given to using a lower-level realistic design earthquake within the remaining life span of the bridge, as the structure is not critical nor experiences high traffic.

This analysis of the bridge was based on the 2012 AASHTO LRFD Bridge Design Specifications using the site-specific response spectra supplied by the geotechnical report from Kleinfelder. However, other engineering literature provides guidelines for a more thorough investigation and analysis existing bridges. Following the recommended analysis guidelines from proven industry resources would help create a refined analysis, and provide recommendations for mitigation of structural deficiencies.

No structural retrofit recommendations are provided without performing a more thorough analysis on the bridge. However, certain deficiencies on the bridge should clearly be addressed and promptly resolved. Investigation of the wood piles under the middle and south pier is required to verify that the piles have not rotten. If the wood piles are rotten, a significant flood would likely undermine the scour-critical piers and cause structural damage and possibly collapse. If the piles are rotten, a retrofit on the footing should be strongly considered. To mitigate undermining the footings during a flood, regardless of the condition of the wood piers, scour protection needs to be provided for the footings. Where spalling has occurred on the bridge as well as structural damage from vehicles, it is recommended that the concrete be repaired and any exposed reinforcement addressed and repaired per governing jurisdiction guidelines.

Because the bridge is listed as a historic landmark, repair and retrofit of the existing bridge would likely be favored by the local community. The bridge design appears to be robust, though maintenance is required to prevent it from falling into further, irreversible disrepair. Repair and a seismic retrofit, if required, would likely extend the life of the bridge, and allow it to be used and enjoyed for years by sightseers, bicyclists, and the agricultural community.

VIII. References

"2010 Fault Activity Map of California." *State of California Department of Conservation.* Accessed 9 September 2013. <http://www.quake.ca.gov/gmaps/FAM/faultactivitymap.html>

AASHTO LRFD Bridge Design Specifications. American Association of State Highway and Transportation Officials, 2012.

"ABAQUS 6.10-EF Documentation." *Simulia.* Accessed 15 April 2013. <http:// server-ifb147.ethz.ch:2080/v6.10ef>

"Bridge Specifications" Structural Bridge Specifications. 18 June 1923.

Center for Engineering Strong Motion Data. US Geological Survey, California Geological Survey & Advanced National Seismic System. Accessed 8 December 2013. <www.strongmotioncenter.org>

Feasibility Study for Stevenson Bridge Road Bridge over Putah Creek. TRC Imbsen, 2007.

Geotechnical Investigation Report, Existing Stevenson Bridge. Kleinfelder. 28 April 2006.

"PEER Ground Motion Database." Pacific Earthquake Engineering Research Center. Accessed 8 December 2013. <http://peer.berkeley.edu/peer_ground_motion_database/spectras/new>

"Reinforced Concrete Bridge Across Putah Creek for Yolo and Solano Counties." Structural Bridge Plans. 18 June 1923.

"Some Useful Numbers." Stanford University course GEOL 615. Accessed 3 August 2013. <www.stanford.edu/~tyzhu/Documents/Some%20Useful%20Numbers.pdf>

"Wood Handbook, Wood as an Engineering Material, Centennial Edition." *United States Department of Agriculture Forest Service.* April 2010.